Title:
Unique In-situ Measurements from Greenland Fjord Show Winter Freshening by Subglacial Melt

Authors:
Karina Hansen1, Nanna B. Karlsson1, Penelope How,1 Ebbe Poulsen2, John Mortensen3, and Søren Rysgaard2.

Affiliations:
1 Department of Glaciology and Climate, Geological Survey of Denmark and Greenland, Copenhagen, Denmark
2 Arctic Research Centre, Department of Biology, Aarhus University, Aarhus, Denmark
3 Greenland Climate Research Centre, Greenland Institute of Natural Resources, Nuuk, Greenland

Correspondence to:
*nbk@geus.dk

Unique In-situ Measurements from Greenland Fjord Show Winter Freshening by Subglacial Melt

Karina Hansen[1], Nanna B. Karlsson[1,*], Penelope How[1], Ebbe Poulsen[2], John Mortensen[3], and Søren Rysgaard[2]

[1]Department of Glaciology and Climate, Geological Survey of Denmark and Greenland, Copenhagen, Denmark

[2]Arctic Research Centre, Department of Biology, Aarhus University, Aarhus, Denmark

[3]Greenland Climate Research Centre, Greenland Institute of Natural Resources, Nuuk, Greenland

[*]nbk@geus.dk

Abstract

The interaction between glacier fronts and ocean waters is one of the key uncertainties for projecting future ice mass loss. Direct observations at glacier fronts are sparse but studies indicate that the magnitude and timing of freshwater fluxes are crucial in determining fjord circulation, ice frontal melt and ecosystem habitability. Particularly wintertime dynamics are severely understudied due to inaccessible conditions leading to a bias towards summer observations. In this study, we present novel in-situ observations of temperature and salinity acquired at the front of a marine-terminating glacier and in surrounding fjords in late winter in Greenland. The observations indicate the existence of an anomalously fresh pool of water by the glacier front. To our knowledge, our study is the first to document the existence of subglacially discharged freshwater outside the summer season, suggesting that meltwater generated at the bed of the glacier discharges into the fjord during winter. Our results have implications for the heat exchange between glacier fronts and ocean waters, glacier frontal melt rates, ocean mixing and currents, and biological production.

Main

In Greenland, marine-terminating glaciers release meltwater at depth causing a mixing of buoyant meltwater and saline ocean water [1, 2]. The discharge of subglacial meltwater and subsequent mixing leads to an upwelling of deep fjord waters close to the glacier fronts, influencing the circulation in the fjord systems [3, 4]. The meltwater impacts glacial frontal melt [5, 6] and ice mélange melt [7], thereby modifying the mass loss from marine-terminating glaciers and consequently glacier contribution to future sea-level rise [8, 9]. The upwelling of subglacial water also impacts the influx and mixing of nutrients [10, 11, 12] by enhancing biological primary productivity, which in turn provides feeding grounds for fish and seabirds [13, 14].

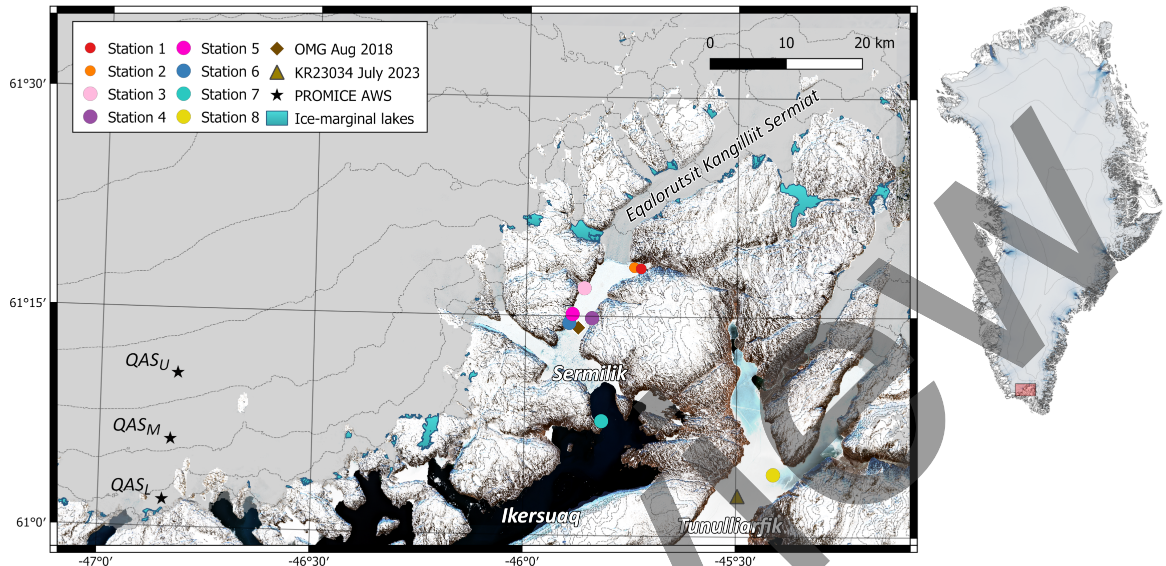

Figure 1: *Eqalorutsit Kangilliit Sermiat and surrounding fjords. The locations of our measurement stations are indicated with coloured circles. Measurements from the OMG project (Oceans Melting Greenland [15]) and the Greenland Institute of Natural Resources (GINR, KR23034) are indicated with a brown diamond and brown triangle, respectively. PROMICE (Programme for Monitoring of the Greenland Ice Sheet) weather stations are marked with black stars. Ice marginal lakes are outlined with turquoise [16] and the ice sheet is coloured grey with 200 m surface topography contours in dashed grey lines from [17, 18]. The background image is from Sentinel 2 (Copernicus Sentinel data, processed by European Space Agency - ESA) from 27th March 2023. The location of the map is indicated on the overview map in red also showing surface topography contours [17, 18] and surface velocities in blue [19].*

Greenland fjords exhibit large seasonal variability in temperature and salinity due to the outflow of glacially-derived freshwater [4, 20]. The melt of snow and ice during the summer months results in large volumes of surface meltwater entering the fjord systems subglacially and as surface runoff. During the summer, subglacial meltwater has been observed in the fjord waters as a layered structure below the summer surface layer via in-situ measurements of temperature and salinity [7]. In contrast, winter measurements of subglacial discharge are effectively unprecedented, and thus the volume of winter subglacial discharge and its impact on fjord systems remains an open question [21]. As a consequence, model estimates of winter subglacial discharge differ by orders of magnitude (cf. [5, 22, 23]). One attempt to measure winter subglacial discharge in Kangersuneq (in Nuup Kangerlua, West Greenland) detected no significant freshwater fluxes [1]. The observations revealed a considerable difference in temperature-salinity profiles between summer and winter, suggesting no noteworthy continuous glacial meltwater outflow during winter. Similar findings have been reported by studies of freshwater discharge during winter in the Milne Fjord epishelf lake in northern Canada, suggesting that winter freshwater discharge is negligible [24]. The observations are in contrast to theoretical estimates of winter freshwater volumes, which suggest that subglacial meltwater discharges into Greenland fjords all year round [22, 23, 25]. Fjord circulation models also disagree on the importance of winter discharge for heat and water exchange (cf. [26, 27]). In the absence of other freshwater fluxes, the discharge of glacial meltwater during winter may have a pronounced influence on fjord dynamics but its impact will depend on water volumes and fjord/glacier settings [21]. This underscores the complexity of bathymetry and heat exchange dynamics between the shelf and marine-terminating glaciers within individual fjords. Finally, the fast-changing Arctic climate may already be causing shifts in wintertime conditions, highlighting the urgency for a better understanding of wintertime dynamics. To our knowledge, our study is the first to measure and document the existence of subglacial freshwater in a fjord during winter shedding light on a hitherto undocumented process.

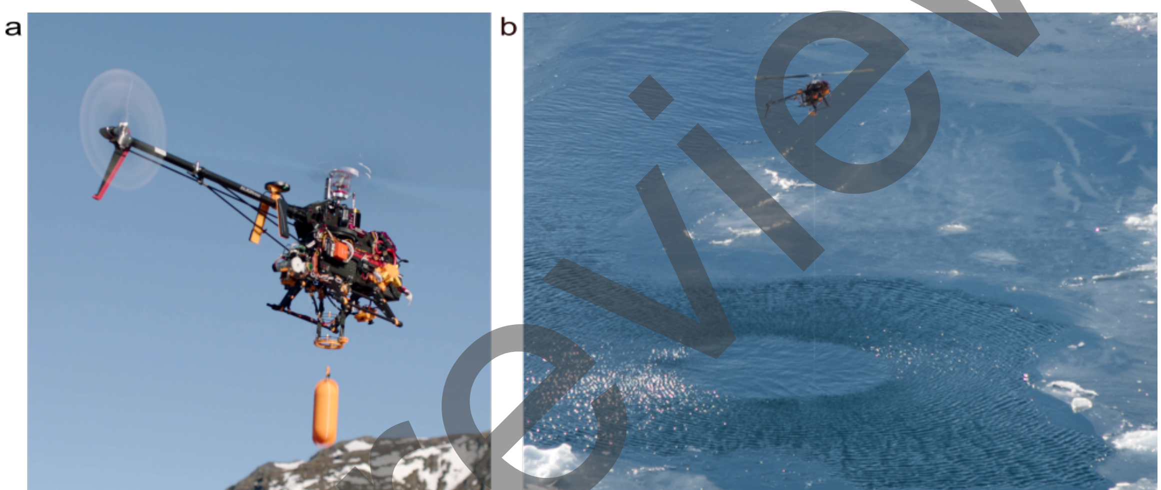

Figure 2: *(a) Complete UAV platform with CTD payload extended. (b) UAV during profiling in a narrow section of open water. Note the line extending from the UAV to the submerged CTD instrument. Photos are from two different deployments, courtesy of Lars Ostenfeld.*

Results

In-situ observations of temperature and salinity

During a dedicated field season in March 2023, we carried out in-situ observations of water properties at Eqalorutsit Kangilliit Sermiat (also at times referred to by its unofficial name Qajuutaap) and neighbouring fjords (Fig. 1). Eqalorutsit Kangilliit Sermiat is one of the largest marine-terminating glaciers in Southwest Greenland with an ice front grounded several hundred metres below sea level. The glacier discharges into an eastern branch of Sermilik Fjord, which forms the inner part of Ikersuaq Fjord (formerly, Bredefjord). The fjord depth ranges from 60 m to 600 m below sea level but bathymetric maps in the middle part of the fjord are highly uncertain due to a lack of in-situ observations.

To retrieve temperature and salinity measurements, we developed and deployed a novel uncrewed aerial vehicle (UAV) solution (Fig. 2). Dense ice mélange has prevented previous studies from acquiring near-front measurements in winter conditions and here the use of the UAV was crucial for our success. The UAV platform consists of a modified kit helicopter with an onboard autonomous winch and a commercial CTD (conductivity, temperature, and depth) sensor payload (see [28] and methods). Its maximum total flight time is 24 minutes, allowing for measurements to be collected up to a distance of 6 km. In addition, we carried out CTD deployments in front of Eqalorutsit Kangilliit Sermiat where flat, walkable, fjord ice enabled us to drill a hole manually in the ice. Finally, the heavy fjord-ice conditions in neighbouring Tunulliarfik Fjord made it possible to drill a hole manually and make additional CTD casts (yellow dot, Fig. 1).

Temperature and salinity data were derived from the CTD profiles, and salinity was calculated using the practical salinity scale (PSS-78). The measurements show that temperature and salinity conditions cluster in three characteristic patterns (Fig. 4): the coldest and freshest conditions were found near the front of Eqalorutsit Kangilliit Sermiat (St. 1 and 2, orange and red lines, respectively), transitioning to slightly warmer and saltier water in the ice mélange (St. 3, 4, 5, 6, rose, magenta, pink, and blue lines, respectively) and Sermilik fjord (St. 7, turquoise lines). Compared to these measurements, conditions in Tunulliarfik fjord (St. 8, yellow line) are warmer and saltier still. For context, we include summer measurements from the OMG (Oceans Melting Greenland) project for August 2018 [29, 15] and from the Greenland Institute of Natural Resources (GINR) for July 2023 (dark and light brown lines, respectively).

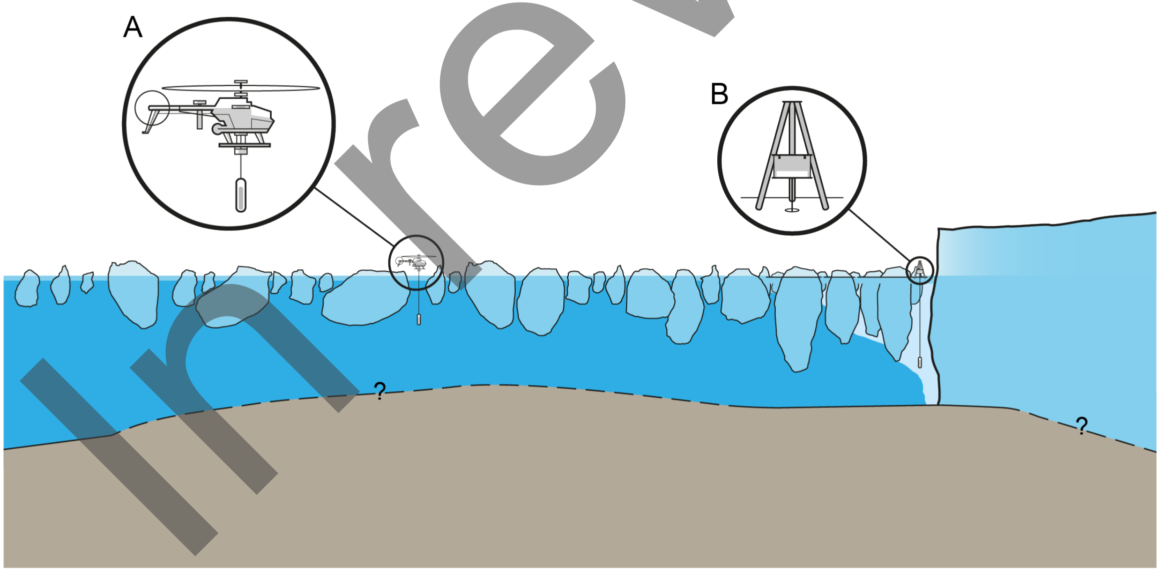

Figure 3: *Schematic of the measurement conditions for the UAV and the manual drill in glacier/ice melange/fjord system. A and B show enlarged versions of our measurement techniques.*

In the *T*-*S*-diagram, St. 1 and St. 2 data show a two-minima temperature profile (black arrows in Fig. 4c). Previous studies have interpreted two-minima temperature profiles as an indication of subglacial discharge [1, 7]. In contrast, two-minima temperature profiles are not seen in our CTD observations from the ice mélange (St. 3-6), nor in Sermilik fjord (St. 7). Rather, the down-fjord observations follow the halocline layer (15-38 m) in the T-S-diagram (Fig. 4c) associated with a melt-line with an observed slope of 2.5∘C per salinity unit, which corresponds to the Gade-slope [30]. The fact that the down-fjord observations follow the halocline layer indicates that the freshening observed more than 5 km from the glacier front can be explained solely by the melting of the ice mélange and stranded icebergs [30]. Fig. 4 also includes a rare winter observation from Nuup Kangerlua in West Greenland acquired ∼ 5 kilometres from the glacier front of Kangiata Nunaata Sermia (black line, retrieved in April 2010 [1], referred to as GF10099). Here, the halocline layer observed below the surface layer (0-17 m depth) is caused by the melting of the ice mélange similar to our down-fjord observations (St. 3-8). Comparison with our St. 1 and St. 2 data highlights the novelty of our observations. Where the surface layer temperature profile of GF10099 follows the freezing point line, St. 1 and 2 profiles do not reach the freezing point line and have local temperature minima, showing a likely input of warmer waters such as a mixture of ambient deep fjord waters and subglacial discharge of meltwater. Based on our observations, we suggest that meltwater enters the fjord subglacially from Eqalorutsit Kangilliit Sermiat, causing the surface layer to freshen. Further, we suggest that the subglacial release of meltwater accumulates under the mélange in front of the glacier in a “fresh surface pool of water” (see Fig. 3) similar to reported epishelf lakes [24].

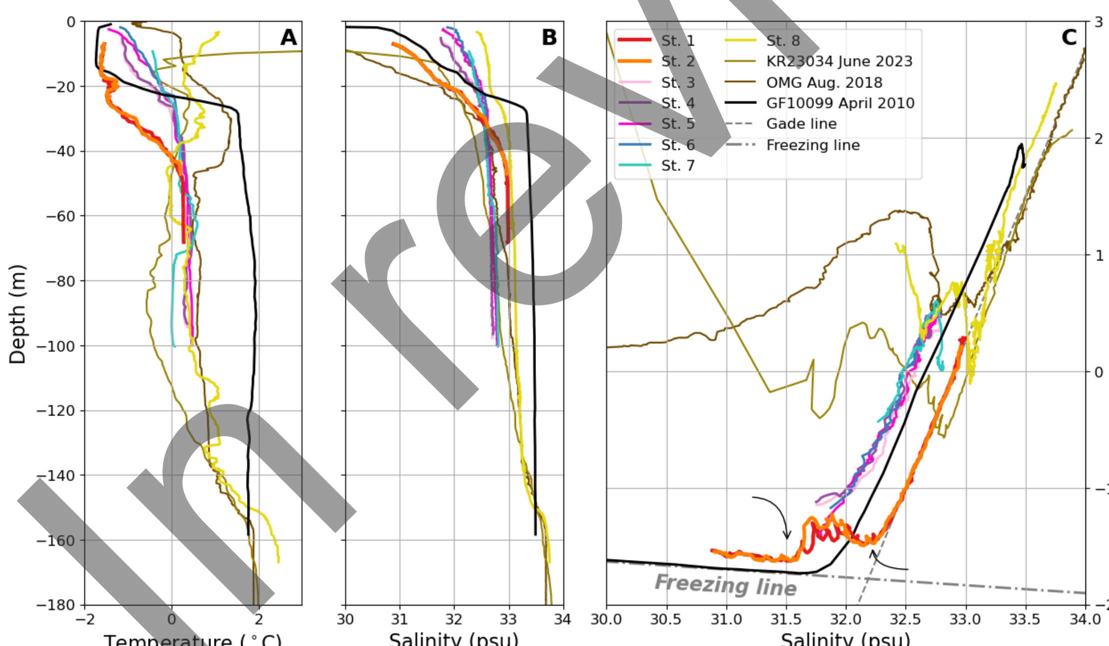

Figure 4: *CTD profiles of temperature (A) and salinity (B), and the corresponding T-S-diagram (C) (locations are shown in Fig. 1). Observations from GINR (KR23034, July 2023) and the OMG project (August 2018) are shown as light and dark brown lines, respectively. A GINR winter observation from Nuup Kangerlua in West Greenland is shown in black (GF10099, April 2010). A melt line with a slope of 2.5° C per salinity unit is indicated with dashed grey lines. The freezing point line of seawater is shown as a dashed-dotted grey line. Black arrows indicate the two-temperature minima seen in St. 1 and 2 data.*

Freshwater volumes and sources

To our knowledge, our study is the first to document the existence of subglacial meltwater accumulation in a fjord during winter. The fact that the freshwater pool is spatially confined is the likely reason why it has not been observed in ice mélanges by previous studies, as the measurements in those studies were retrieved more than one kilometre from the glacier front [31, 1]. The two-minima signal in our data is not as strong as observed during summer conditions [4] indicating that the subglacial discharge may not be very large.

Subglacial water may have different provenance. During the summer, subglacially discharged water is derived predominantly from surface meltwater that enters the subglacial system via moulins and crevasses [32]. During winter, in the absence of surface melt, the origin of the water is less clear. We suggest that the observed pool of meltwater originates from basal melting, in other words, from melting at the interface between ice and bedrock. At present, only a few deep drill sites have measured basal conditions of the Greenland ice sheet directly [33, 34] but indirect estimates combined with numerical models show that large parts of the base of the ice sheet are at the melting point [35]. Importantly, because the basal melt is predominantly caused by heat from friction and geothermal flux [36], studies suggest that basal meltwater discharges into the fjords during all seasons [22, 36, 25] (see also methods). Thus, basal meltwater is a potential source of wintertime freshwater.

Two other freshwater sources may also cause subglacial discharge: surface melt and glacier-lake drainage events. Here, we outline why we discard these two meltwater sources as potential explanations for our measurements. Firstly, while large volumes of surface meltwater enter the fjord at Eqalorutsit Kangilliit Sermiat in the summertime, the winter surface melt volume is orders of magnitude smaller due to low air temperatures (see Fig. S1). We estimate the likely surface melt using an improved Positive Degree Day model [37] and in-situ measurements from the Automatic Weather Stations (AWS, [38]) situated approximately 80 km to the west of Eqalorutsit Kangilliit Sermiat (Fig. 1) (see methods). Our results indicate that surface melt (i.e., where air temperatures exceeded 0°C) occurred at low elevations for two days in early March (see Fig. S2). The daily melt rate at the lowest-elevation AWS was 5.6 mm and 6.4 mm on 2nd and 3rd March, respectively (three weeks before our measurements began). No surface melt was recorded at the AWS at 600 m or 900 m elevation. Given the small volume of meltwater generated, we posit that the water is unlikely to have penetrated to the bed of the glacier and that the majority of the water was retained and refrozen close to the ice surface, either in the broken and weathered bare-ice surface or in snow pockets [39]. This is supported by observational evidence of refrozen ice, snow pockets and dry crevasses at the glacier margin (see Fig. S3).

A second freshwater source is the drainages of ice-marginal lakes that can occur at any time of year. To constrain freshwater volumes from ice-marginal lakes, we investigated 21 lakes that share a margin with the glacier's catchment area (mapped in 2017 by [16]). Of the 21 ice-marginal lakes that exist around the lateral margins of Eqalorutsit Kangilliit Sermiat, five lakes could be identified between January and April 2023. Little is known about the dynamics of these lakes, however, visual inspection and classification through satellite images suggest that the lakes had limited variability in their areas between January and April 2023. There is no evidence of glacial lake outburst floods or full drainage events during the monitoring period (see methods).

To our knowledge, our study is the first to successfully measure basal meltwater at a glacier front. For Eqalorutsit Kangilliit Sermiat, the estimated monthly basal melt volume is 3.8×10^6 m^3 corresponding to 2 % of the glacier's annual mass loss (Karlsson and others, 2023). This estimate is highly uncertain and we leverage our CTD observations to evaluate the amount of freshwater necessary to cause the observed freshening. Our results indicate a freshwater volume corresponding to 2.4×10^5 m^3 is needed (see methods), which is an order of magnitude lower than the theoretically estimated monthly basal melt. We suggest two reasons for this discrepancy that are not mutually exclusive. Firstly, the source area for the basal meltwater is reconstructed based on surface and bed topography where the latter has uncertainties upwards of 300 m [17]. It is therefore possible that the source area is smaller than estimated, which would lower the volume of basal meltwater discharging at the glacier front. Secondly, some basal meltwater may be retained in the subglacial system. Studies have shown that the subglacial system can shut down during the winter [40, 41]. The shutdown could block the transport of basal meltwater from upstream parts of the glacier basin until such a time when surface meltwater volumes reactivate the subglacial water transport system. This potential disconnection between parts of the subglacial system may be highly dependent on ice-flow velocities and the glacier's topographic setting.

Impact of winter meltwater discharge on fjord heat budget, salt budget and ecosystem

Our measurements indicate that basal meltwater released subglacially during the winter modifies near-glacier water properties and influences processes controlling ice/fjord interactions, fjord dynamics and ecosystems.

The winter subglacial discharge from Eqalorutsit Kangilliit Sermiat likely leads to a replenishment of nutrients in the surface waters thereby readying the system for an expansive primary production during spring when the ice mélange breaks up. Hence, winter subglacial discharge in the inner parts of fjords may play a more important role in priming the spring phytoplankton production than previously anticipated. It has been reported that the spring bloom in a marine-terminating glacier fjord will be triggered by out-fjord winds and coastal inflows driving an upwelling in the inner part of the fjord during spring, hereby supplying nutrient-rich water to the surface layer [42]. Our observations suggest that subglacial discharge during winter may entrain nutrients from deeper waters and accumulate them in a surface pool of water beneath the ice mélange near the glacier front. As a result, favourable conditions for a spring phytoplankton bloom are established when the mélange breaks up. It is noteworthy that the spring bloom might not occur directly in front of the glacier but further out in the fjord, as the nutrient pool will track the drifting ice pushed by prevailing winds from the northeast during spring (see observed wind directions in Fig. S6). This further underscores the seasonal significance of marine-terminating glaciers in stimulating primary production.

Observations and models suggest that subglacial discharge causes fjord circulation patterns leading to a renewal of fjord basin waters over seasonal time scales [2, 43]. Although melt from icebergs and ice mélange probably dominates the winter freshwater budget for most ice-filled fjords [44] any inflow of glacial freshwater may be of physical and biogeochemical significance [21]. Nevertheless, most fjord circulation models focus on summertime dynamics as they aim to understand processes occurring during the peak meltwater season [45, 46]. In the near future, increasing Arctic temperatures are likely to lead to a speed-up of Greenland glaciers [47] and consequently an increase in basally-generated meltwater due to increased friction [36] and thereby also an increased winter freshwater discharge. Thus there is an urgent need to understand the role and impact of winter subglacial discharge on fjord dynamics.

Our unique observations of winter subglacial discharge highlight the importance of this severely understudied freshwater source and demonstrate the potential of UAV-supported observations during the Arctic winter. The potentially disproportionately large influence of winter subglacial discharge on fjord waters, coupled with its ability to enhance spring primary production, emphasises the significant impact marine-terminating glaciers can exert on fjord waters, fjord circulation and not least ecosystem productivity with consequences for fisheries in the coastal zone surrounding Greenland.

Methods

UAV technology

Crewed aircraft have been used previously to study fjord conditions by employing expendable XCTD instruments [48, 7, 31]. However, the method is constrained by the cost of aircraft hire and equipment replacement, as well as the fact that precise deployment within narrow openings in fjord ice is challenging. To alleviate these issues, we developed a novel uncrewed aerial vehicle (UAV) solution (Fig. 2). A complete description of the UAV including hardware description, cost overview, and assembly and deployment instructions is available in [28].

The UAV is based on a modified Align Trex 650X kit helicopter with an autopilot system and a custom payload attached. The autopilot provides autonomous flight capabilities along with pilot assistance when manually operating the UAV. The UAV payload consists of a SonTek CastAway CTD sensor, a winch unit, and an HD camera attached to a gimbal. Control, telemetry, and video transmission are handled by the Herelink HD Video system with a tested range of 6 km. The winch unit consists of a winch motor, that reels the CTD in and out, and a pivot mechanism. This mechanism transitions the sensor from horizontal during takeoff, cruise and landing to vertical during profiling. Once vertical, the sensor is lowered by the winch motor. A range of servo motors is used to control the pivot mechanism and gimbal and to engage and disengage the winch motor for the different stages of operation. The complete system is powered by a 22.2 V 14 Ah lithium polymer battery pack that is insulated and preheated before deployment to improve performance in cold environments.

The takeoff weight of the complete UAV platform is 6.5 kg with a length of 1.145 m and a rotor diameter of 1.455 m. The maximum tested cruise speed is 16 m s^{-1}. All components, including batteries, controller, and CTD payload, can be packed in a 1.400x450x250 mm Zarges box for shipping and handling. During fieldwork, the UAV was transported within the cabin of an AS350 helicopter with two crew and three passengers. The total cost of the UAV platform with the CTD sensor is €13,000.

Basal melt estimate

The basal melt estimate presented here is based on already published [25] based on methods developed in [36]. We briefly summarise the methods here and refer readers to the original study for more details. The basal melt rates b_m are calculated based on estimates of available heat sources (E)

$$b_m = E/(\rho L)$$

Where ρ is ice density and L is the latent heat of fusion. In the absence of surface melt, the basal meltwater derives from heat generated by friction heat and the geothermal flux [36]. Using subglacial drainage catchments derived from the hydropotential [49] based on surface and bed topography from BedMachine v5 [17], the basal melt is routed to the front of the glacier. Results show that the average monthly basal melt volume in March is 3.8×10^6 m^3 based on 2010-2020 averages [25]. This assumes that all melt generated at the bed is immediately transported to the front of the glacier and does not account for the possibility of subglacial storage or delays in subglacial transport efficiency.

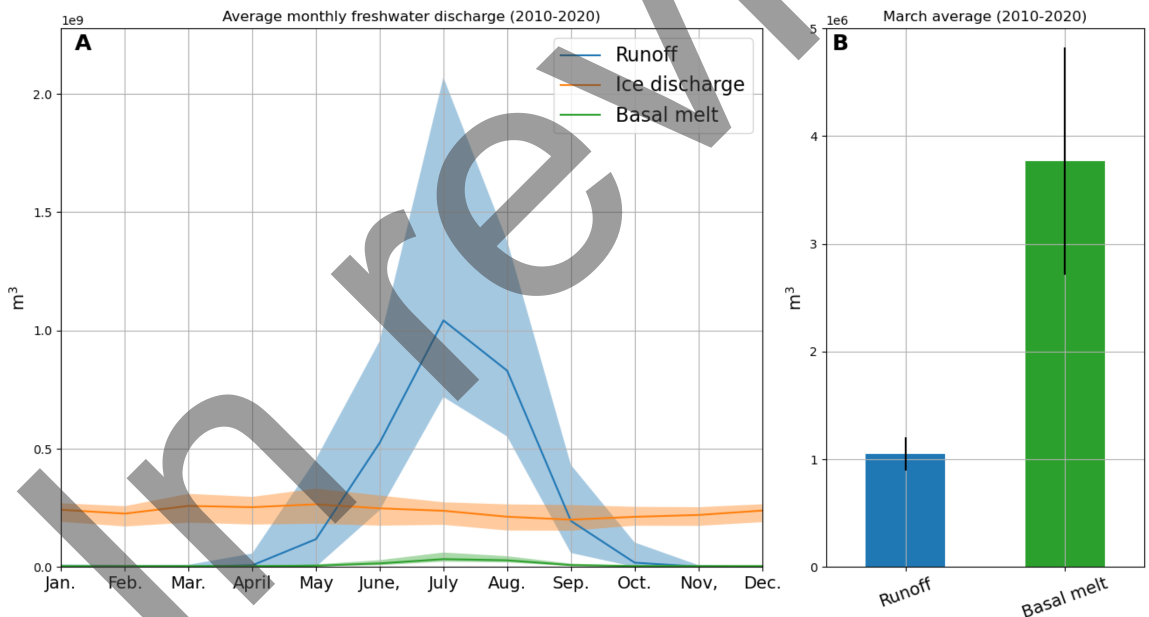

Figure S1: *Average monthly freshwater fluxes for Eqalorutsit Kangilliit Sermiat 2010-2020 [25]. In (A) the shaded areas indicate the range of values that occurred during 2010-2020. In (B) errorbars show the uncertainty associated with the average values for runoff and basal melt for March.*

Estimates of surface runoff

The winter surface melt at elevations 280 m, 600 m and 900 m was estimated using an improved Positive Degree Day (PDD) model that accounts for the time lag in the melt that occurs when the air temperature is above 0℃ while the temperature of the ice surface is not yet at the melting point (Tsai and Ruan, 2018). We combine the model with measurements from the AWS PROMICE stations QAS_L, QAS_M and QAS_U [38, 50]. In this study, daily air and surface temperatures are used as model input. The improved PDD model contains a function for estimating surface temperature from air temperature but comparisons of the modelled surface temperatures with data from the AWSs showed that the model performance relies heavily on initial parameter settings. Thus we have used measured surface temperatures where available. During the period of interest, air and surface temperature measurements are available from the AWSs at 280 m and 900 m elevation. There are no surface temperature measurements from the AWSs at 600 m elevation, and to avoid the parameterisation bias in the PDD model we instead estimate the surface temperature using a linear regression model, which is trained on earlier measurements of air and surface temperature. Simple validation of the linear regression model indicates that the linear regression performs well with a Mean Squared Error of 1.16 and an R-squared value of 0.97.

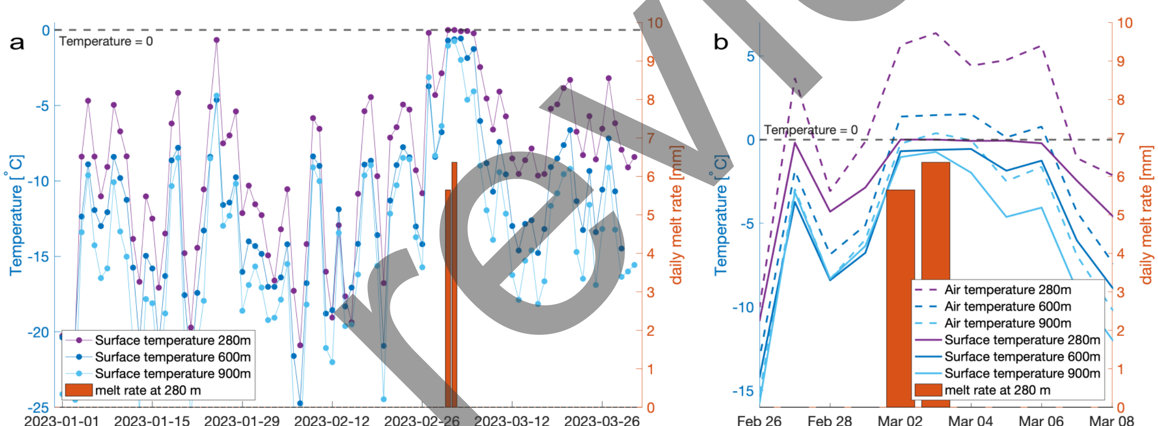

Figure S2: *Temperature time series at elevations 280 m, 600 m and 900 m by AWS approx. 80 km west of Eqalorutsit Kangilliit Sermiat and the modelled daily melt rate [37]. (a) Time series from 2023-01-01 to 2023-04-01 (b) Zoom of (a) during the high-temperature period at the beginning of March 2023 with air temperatures included.*

We use the improved PDD to estimate surface melt, based on the observed (for 280 m and 900 m elevations) or reconstructed (for 600 m elevation) surface temperatures. The results show that of the three sites, surface melt only occurs at the lowest elevation site. The melt rate at the lowest-elevation AWS is 5.6 mm/day and 6.4 mm/day on the 2nd and 3rd of March, respectively (Fig. S2). No surface melt was recorded at the AWS at 600 m or 900 m elevation. While we cannot rule out that some of the surface meltwater penetrated to the bed of the glacier and mixed with the basal meltwater, we consider this to be unlikely for the following reasons. Firstly, visual inspection of the glacier surface during our field campaign revealed dry crevasses (Fig. S3a), icicles (Fig. S3S4b), refrozen puddles of water (Fig. S3c) and snow pockets on the surface (Fig. S3d); all suggesting that water forming on the surface refreezes again. Secondly, previous studies suggest that meltwater can be stored and refrozen in the weathered glacier surface and the surface snow [39]. Finally, scrutiny of remote sensing images showed no evidence of surface water transport or drainage systems.

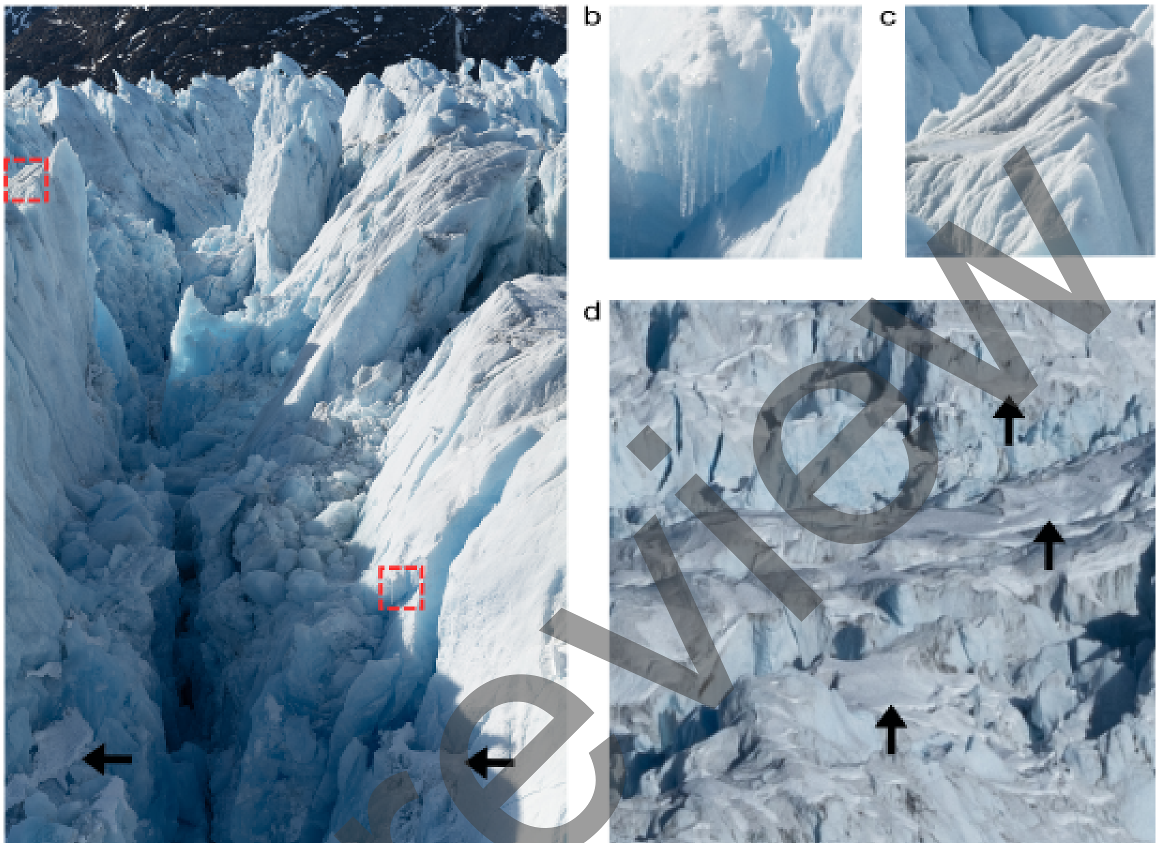

Figure S3: *Pictures of Eqalorutsit Kangilliit Sermiat taken from a helicopter by Lars Ostenfeld on the 27th of March 2023. (a) Crevasse photographed from the side. The red squares show the location of b and c. The black arrows point to some of the snow pockets. (b) Magnification of icicles in a. (c) Magnification of a refrozen puddle of water in a. (d) Glacier surface photographed from above. The black arrows point to some of the snow pockets.*

Ice-marginal lake change

A time series of surface areas was derived for the five ice-marginal lakes identified between January and April 2023 (Fig. S4a). The five lakes were delineated manually across 21 timesteps using GEEDit [51]. Our dataset consists of 17 scenes from Sentinel-2 (10 m spatial resolution) and 6 scenes from Landsat 9 (30 m spatial resolution) and all scenes had less than 50% cloud cover (Fig. S4b). Occlusion of lake outlines occurred in some scenes due to localized cloud cover. The error estimate in lake surface area was quantified by repeated manual delineation of the Nordbosø lake from the first Sentinel-2 and Landsat 9 image in the time series; returning an error estimate of ±4.5% and ±6.3%, respectively. The time series presented in Fig. S4b suggests that the five ice-marginal lakes in this region experienced limited variability in the areas between January and April 2023. There is also no evidence of any glacier lake outburst flood or full drainage events from the five lakes. The highest variability in surface lake area is evident at the beginning of the time-series record, which likely reflects the high snow cover at the beginning of the year. Generally, the variability in lake areas is low in the latter half of the time series, coinciding with higher data coverage, particularly from the Sentinel-2 record. The smaller lakes exhibit small changes across the time series; for example, Lake 1644 had a mean surface area of 0.23 km^2, varying between 0.19 km^2 (Sentinel-2 delineation) and 0.29 km^2 (Landsat 9 delineation), and a standard deviation of 0.03. Nordbosø Lake (lake ID 1897) exhibits the largest changes, primarily reflecting its size relative to the other lakes presented here. Lake area is stable and consistent during our field campaign and the month preceding, with an average standard deviation of 0.062 in March (compared to an average standard deviation of 0.166 over the entire time series). We thus conclude that there is no evidence of ice-marginal lake drainage in our study area.

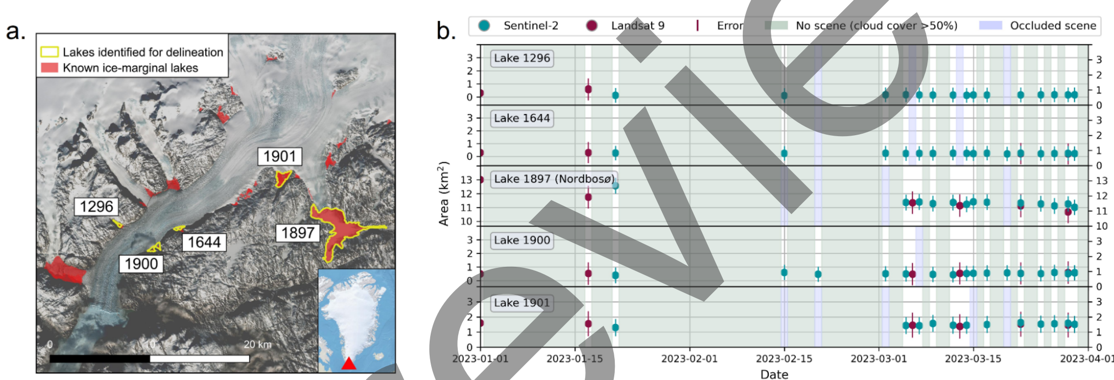

Figure S4: *The five ice-marginal lakes identified between January and April 2023 within the Eqalorutsit Kangilliit Sermiat catchment area (a) and the corresponding time-series of lake area change from Sentinel-2 and Landsat 9 imagery (b). Known ice-marginal lakes and lake identification numbers follow those defined by the 2017 inventory of Greenland ice-marginal lakes [16]. The background image in (a) is a visible composite from Sentinel-2 imagery captured on 6th March 2023.*

Freshwater pool extent and volume

We estimate the size of the under-ice freshwater pool by assuming that the pool extends across the entire glacier front but does not extend to our measurement at St. 3. The size of the pool is outlined in Fig. S5 and estimated at 14 km^2 area. Assuming that the under-ice lake has uniform salinity conditions similar to those measured at St. 1 and St. 2, we can calculate the amount of freshwater by integrating the difference between the average salinity profile of St. 1 and St. 2 and the average salinity profiles from St. 3 and St. 4 down to 32 m depth where profiles connect (Fig. 4). The under-ice lake freshwater reservoir amounts to 2.38×10^5 m^3 which is an order of magnitude smaller than the theoretically estimated monthly subglacial discharge due to basal melt.

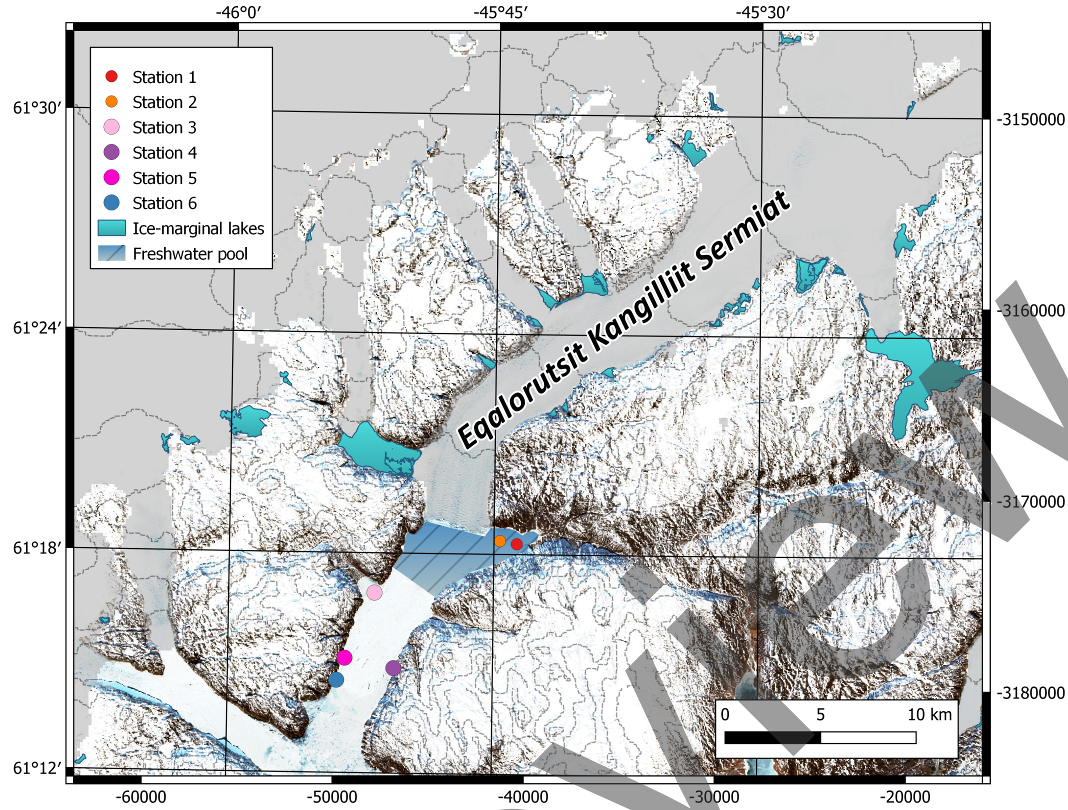

Figure S5: *Map of Eqalorutsit Kangilliit Sermiat and surrounding areas. The suggested extent of the under-ice freshwater pool is indicated in dashed blue.*

Prevailing wind direction

Fig. S6 shows the measured wind directions from AWSs QAS_L and QAS_U from August 2009 to early 2024. As shown, the prevailing wind direction is from the northeast.

Figure S6: *Daily wind directions from* QAS_L *and* QAS_U *from 2009 to January 2024.*

Acknowledgements

This work was supported by a Villum Experiment project to NBK from the Villum Foundation (project no. 40858). Further support was provided by PROMICE, funded by the Geological Survey of Denmark and Greenland (GEUS) and the Danish Ministry of Climate, Energy and Utilities under the Danish Cooperation for Environment in the Arctic (DANCEA), conducted in collaboration with DTU Space (Technical University of Denmark) and Asiaq Greenland Survey. The development of the UAV was supported by Aage V Jensens Foundations to the project "Greenland gradients Flagship project". PH was supported by an ESA Living Planet Fellowship (4000136382/21/I-DT-lr) entitled "Examining Greenland's Ice Marginal Lakes under a Changing Climate". We thank Baptiste Vandecrux (GEUS) for advice and insightful discussions on calculating surface melt. The skilled and patient employees of the Department of Biology mechanical and electrical workshops are acknowledged for their significant contributions during the design and build of the ARC-AWS. We acknowledge the helpful community of ArduPilot and Bill Geyer for support and guidance during UAV development. Egon R. Frandsen is acknowledged for logistical support during fieldwork. We thank the pilots from SERMEQ helicopters for their support and enthusiasm during the 2023 fieldwork.

Author contributions statement

NBK conceived of the study in collaboration with SR. KH managed the project and planned the fieldwork campaign. EP developed the UAV solution with input from SR. EP, SR, KH and NBK collected the data and analysed it with input from JM. KH calculated surface melt rates. PH compiled and analysed the ice-marginal lake observations. NBK, SR and KH led the writing of the article with contributions from all authors. NBK and SR acquired the funding for the work. All authors reviewed the manuscript.

Additional information

Data availability The measurements acquired in March 2023 and the GINR measurement KR23034 are available at the GEUS Dataverse DOI: 10.22008/FK2/UHV7FF.

Competing interests The authors declare that they have no competing interests.

References

[1] Mortensen, J., Bendtsen, J., Motyka, R. J., Lennert, K., Truffer, M., Fahnestock, M. & Rysgaard, S. On the seasonal freshwater stratification in the proximity of fast-flowing tidewater outlet glaciers in a sub-Arctic sill fjord. *Journal of Geophysical Research: Oceans* **118**, 1382–1395 (2013).

[2] Carroll, D., Sutherland, D. A., Shroyer, E. L., Nash, J. D., Catania, G. A. & Stearns, L. A. Modeling Turbulent Subglacial Meltwater Plumes: Implications for Fjord-Scale Buoyancy-Driven Circulation. *Journal of Physical Oceanography* 2169–2185 (2015).

[3] Straneo, F. & Cenedese, C. The Dynamics of Greenland's Glacial Fjords and Their Role in Climate. *Annual Review of Marine Science* **7**, 89–112 (2015).

[4] Mortensen, J., Bendtsen, J., Lennert, K. & Rysgaard, S. Seasonal variability of the circulation system in a west Greenland tidewater outlet glacier fjord, Godthåbsfjord (64 N). *Journal of Geophysical Research: Earth Surface* **119**, 2591–2603 (2014).

[5] Rignot, E., Xu, Y., Menemenlis, D., Mouginot, J., Scheuchl, B., Li, X., Morlighem, M., Seroussi, H., den Broeke, M. v., Fenty, I. *et al.* Modeling of ocean-induced ice melt rates of five west Greenland glaciers over the past two decades. *Geophysical Research Letters* **43**, 6374–6382 (2016).

[6] Jackson, R., Nash, J., Kienholz, C., Sutherland, D., Amundson, J., Motyka, R., Winters, D., Skyllingstad, E. & Pettit, E. Meltwater intrusions reveal mechanisms for rapid submarine melt at a tidewater glacier. *Geophysical Research Letters* **47**, e2019GL085335 (2020).

[7] Mortensen, J., Rysgaard, S., Bendtsen, J., Lennert, K., Kanzow, T., Lund, H. & Meire, L. Subglacial discharge and its down-fjord transformation in West Greenland fjords with an ice mélange. *Journal of Geophysical Research: Oceans* **125**, e2020JC016301 (2020).

[8] Beckmann, J., Perrette, M., Beyer, S., Calov, R., Willeit, M. & Ganopolski, A. Modeling the response of Greenland outlet glaciers to global warming using a coupled flow line–plume model. *The Cryosphere* **13**, 2281–2301 (2019). URL `https://www.the-cryosphere.net/13/2281/2019/`.

[9] Slater, D. A., Felikson, D., Straneo, F., Goelzer, H., Little, C. M., Morlighem, M., Fettweis, X. & Nowicki, S. Twenty-first century ocean forcing of the Greenland ice sheet for modelling of sea level contribution. *The Cryosphere* **14**, 985–1008 (2020). URL `https://tc.copernicus.org/articles/14/985/2020/`.

[10] Meire, L., Mortensen, J., Meire, P., Juul-Pedersen, T., Sejr, M. K., Rysgaard, S., Nygaard, R., Huybrechts, P. & Meysman, F. J. Marine-terminating glaciers sustain high productivity in Greenland fjords. *Global Change Biology* **23**, 5344–5357 (2017).

[11] Kanna, N., Sugiyama, S., Ohashi, Y., Sakakibara, D., Fukamachi, Y. & Nomura, D. Upwelling of Macronutrients and Dissolved Inorganic Carbon by a Subglacial Freshwater Driven Plume in Bowdoin Fjord, Northwestern Greenland. *Journal of Geophysical Research: Biogeosciences* **123**, 1666–1682 (2018).

[12] Hopwood, M. J., Carroll, D., Dunse, T., Hodson, A., Holding, J. M., Iriarte, J. L., Ribeiro, S., Achterberg, E. P., Cantoni, C., Carlson, D. F., Chierici, M., Clarke, J. S., Cozzi, S., Fransson, A., Juul-Pedersen, T., Winding, M. H. & Meire, L. Review article: How does glacier discharge affect marine biogeochemistry and primary production in the Arctic? *Cryosphere* **14**, 1347–1383 (2020).

[13] Hopwood, M. J., Carroll, D., Browning, T. J., Meire, L., Mortensen, J., Krisch, S. & Achterberg, E. P. Non-linear response of summertime marine productivity to increased meltwater discharge around Greenland. *Nature Communications* **9** (2018).

[14] Nishizawa, B., Kanna, N., Abe, Y., Ohashi, Y., Sakakibara, D., Asaji, I., Sugiyama, S., Yamaguchi, A. & Watanuki, Y. Contrasting assemblages of seabirds in the subglacial meltwater plume and oceanic water of Bowdoin Fjord, northwestern Greenland. *ICES Journal of Marine Science* **77**, 711–720 (2019). URL `https://doi.org/10.1093/icesjms/fsz213`. `https://academic.oup.com/icesjms/article-pdf/77/2/711/32881925/fsz213.pdf`.

[15] Fenty, I., Willis, J. K., Khazendar, A., Dinardo, S., René, Fukumori, I., Holland, D., Jakobsson, M., Moller, D., Morison, J., Münchow, A., Rignot, E., Schodlok, M., Thompson, A. F., Tinto, K., Rutherford, M. & Trenholm, N. Oceans Melting Greenland: Early Results from NASA's Ocean-Ice Mission in Greenland. *Oceanography* **29** (2016). URL `https://doi.org/10.5670/oceanog.2016.100`.

[16] How, P., Messerli, A., Mätzler, E., Santoro, M., Wiesmann, A., Caduff, R., Langley, K., Bojesen, M. H., Paul, F., Kääb, A. *et al.* Greenland-wide inventory of ice marginal lakes using a multi-method approach. *Scientific reports* **11**, 4481 (2021).

[17] Morlighem, M., Williams, C. N., Rignot, E., An, L., Arndt, J. E., Bamber, J. L., Catania, G., Chauché, N., Dowdeswell, J. A., Dorschel, B., Fenty, I., Hogan, K., Howat, I., Hubbard, A., Jakobsson, M., Jordan, T. M., Kjeldsen, K. K., Millan, R., Mayer, L., Mouginot, J., Noël, B. P. Y., O'Cofaigh, C., Palmer, S., Rysgaard, S., Seroussi, H., Siegert, M. J., Slabon, P., Straneo, F., van den Broeke, M. R., Weinrebe, W., Wood, M. & Zinglersen, K. B. BedMachine v3:

Complete Bed Topography and Ocean Bathymetry Mapping of Greenland From Multibeam Echo Sounding Combined With Mass Conservation. *Geophysical Research Letters* **44**, 11,051–11,061 (2017).

[18] Morlighem, M. e. a. IceBridge BedMachine Greenland, Version 5 (2022). URL `https://nsidc.org/data/IDBMG4/versions/5`.

[19] Solgaard, A., Messerli, A., Schellenberger, T., Hvidberg, C., Grinsted, A., Jackson, M., Zwinger, T., Karlsson, N. & Dahl-Jensen, D. Basal conditions at Engabreen, Norway, inferred from surface measurements and inverse modelling. *Journal of Glaciology* **64** (2018).

[20] Jackson, R. H., Straneo, F. & Sutherland, D. A. Externally forced fluctuations in ocean temperature at Greenland glaciers in non-summer months. *Nature Geoscience* **7**, 503–508 (2014).

[21] Vonnahme, T. R., Nowak, A., Hopwood, M. J., Meire, L., Søgaard, D. H., Krawczyk, D., Kalhagen, K. & Juul-Pedersen, T. Impact of winter freshwater from tidewater glaciers on fjords in Svalbard and Greenland; A review. *Progress in Oceanography* **219**, 103144 (2023). URL `https://www.sciencedirect.com/science/article/pii/S0079661123001878`.

[22] Cook, S. J., Swift, D. A., Kirkbride, M. P., Knight, P. G. & Waller, R. I. The empirical basis for modelling glacial erosion rates. *Nature Communications* **11** (2020).

[23] Sommers, A., Meyer, C., Morlighem, M., Rajaram, H., Poinar, K., Chu, W. & Mejia, J. Subglacial hydrology modeling predicts high winter water pressure and spatially variable transmissivity at Helheim Glacier, Greenland. *Journal of Glaciology* 1–13 (2023).

[24] Hamilton, A. K., Mueller, D. & Laval, B. E. Ocean Modification and Seasonality in a Northern Ellesmere Island Glacial Fjord Prior to Ice Shelf Breakup: Milne Fiord. *Journal of Geophysical Research: Oceans* **126**, e2020JC016975 (2021). E2020JC016975 2020JC016975.

[25] Karlsson, N. B., Mankoff, K. D., Solgaard, A. M., Larsen, S. H., How, P. R., Fausto, R. S. & Sørensen, L. S. A data set of monthly freshwater fluxes from the Greenland ice sheet's marine-terminating glaciers on a glacier–basin scale 2010–2020. *GEUS Bulletin* **53** (2023). URL `https://geusbulletin.org/index.php/geusb/article/view/8338`.

[26] Fraser, N. J., Inall, M. E., Magaldi, M. G., Haine, T. W. N. & Jones, S. C. Wintertime Fjord-Shelf Interaction and Ice Sheet Melting in Southeast Greenland. *Journal of Geophysical Research: Oceans* **123**, 9156–9177 (2018).

[27] Hager, A. O., Sutherland, D. A. & Slater, D. A. Local forcing mechanisms challenge parameterizations of ocean thermal forcing for Greenland tidewater glaciers. *The Cryosphere* **18**, 911–932 (2024).

[28] Poulsen, E., Rysgaard, S., Hansen, K. & Karlsson, N. B. Uncrewed aerial vehicle with onboard winch system for rapid, cost-effective, and safe oceanographic profiling in hazardous and inaccessible areas. *HardwareX* **18**, e00518 (2024).

[29] OMG. 2020. OMG CTD Conductivity Temperature Depth. Ver. 1. Dataset accessed [2023-12-18].

[30] Gade, H. G. Melting of Ice in Sea Water: A Primitive Model with Application to the Antarctic Ice Shelf and Icebergs. *Journal of Physical Oceanography* **9**, 189 – 198 (1979).

[31] Straneo, F., Curry, R. G., Sutherland, D. A., Hamilton, G. S., Cenedese, C., Våge, K. & Stearns, L. A. Impact of fjord dynamics and glacial runoff on the circulation near Helheim Glacier. *Nature Geoscience* **4**, 322–327 (2011).

[32] Hoffman, M. J., Andrews, L. C., Price, S. F., Catania, G. A., Neumann, T. A., Lüthi, M. P., Gulley, J., Ryser, C., Hawley, R. L. & Morriss, B. Greenland subglacial drainage evolution regulated by weakly connected regions of the bed. *Nature Communications* **9** (2016).

[33] Ryser, C., Lüthi, M. P., Andrews, L. C., Hoffman, M. J., Catania, G. A., Hawley, R. L., Neumann, T. A. & Kristensen, S. S. Sustained high basal motion of the Greenland ice sheet revealed by borehole deformation. *Journal of Glaciology* **60**, 647–660 (2014).

[34] Dahl-Jensen, D., Albert, M. R., Aldahan, A., Azuma, N., Balslev-Clausen, D., Baumgartner, M., Berggren, A.-M., Bigler, M., Binder, T., Blunier, T., Bourgeois, J. C., Brook, E. J., Buchardt, S. L., Buizert, C., Capron, E., Chappellaz, J., Chung, J., Clausen, H. B., Cvijanovic, I., Davies, S. M., Ditlevsen, P., Eicher, O., Fischer, H., Fisher, D. A., Fleet, L. G., Gfeller, G., Gkinis, V., Gogineni, S., Goto-Azuma, K., Grinsted, A., Gudlaugsdottir, H., Guillevic, M., Hansen, S. B., Hansson, M., Hirabayashi, M., Hong, S., Hur, S. D., Huybrechts, P., Hvidberg, C. S., Iizuka, Y., Jenk, T., Johnsen, S. J., Jones, T. R., Jouzel, J., Karlsson, N. B., Kawamura, K., Keegan, K., Kettner, E., Kipfstuhl, S., Kjær, H. A., Koutnik, M., Kuramoto, T., Köhler, P., Laepple, T., Landais, A., Langen, P. L., Larsen, L. B., Leuenberger, D., Leuenberger, M., Leuschen, C., Li, J., Lipenkov, V., Martinerie, P., Maselli, O. J., Masson-Delmotte, V., McConnell, J. R., Miller, H., Mini, O., Miyamoto, A., Montagnat-Rentier, M., Mulvaney, R., Muscheler, R., Orsi, A. J., Paden, J., Panton, C., Pattyn, F., Petit, J.-R., Pol, K., Popp, T., Possnert, G., Prié, F., Prokopiou, M., Quiquet, A., Rasmussen, S. O., Raynaud, D., Ren, J., Reutenauer, C., Ritz, C., Röckmann, T., Rosen, J. L., Rubino, M., Rybak, O., Samyn, D., Sapart, C. J., Schilt, A., Schmidt, A. M. Z., Schwander, J., Schüpbach, S., Seierstad, I., Severinghaus, J. P., Sheldon, S., Simonsen, S. B., Sjolte, J., Solgaard, A. M., Sowers, T., Sperlich, P., Steen-Larsen, H. C., Steffen, K., Steffensen, J. P., Steinhage, D., Stocker, T. F., Stowasser, C., Sturevik, A. S., Sturges, W. T., Sveinbjörnsdottir, A., Svensson, A., Tison, J.-L., Uetake, J., Vallelonga, P., van de Wal, R. S. W., van der Wel, G., Vaughn, B. H., Vinther, B., Waddington, E., Wegner, A., Weikusat, I., White, J. W. C., Wilhelms, F., Winstrup, M., Witrant, E., Wolff, E. W., Xiao, C. & Zheng, J. Eemian interglacial reconstructed from a Greenland folded ice core. *Nature* **493**, 489–494 (2013).

[35] MacGregor, J. A., Chu, W., Colgan, W. T., Fahnestock, M. A., Felikson, D., Karlsson, N. B., Nowicki, S. M. J. & Studinger, M. GBaTSv2: a revised synthesis of the likely basal thermal state of the Greenland Ice Sheet. *The Cryosphere* **16**, 3033–3049 (2022).

[36] Karlsson, N. B., Solgaard, A. M., Mankoff, K. D., Gillet-Chaulet, F., MacGregor, J. A., Box, J. E., Citterio, M., Colgan, W. T., Larsen, S. H., Kjeldsen, K. K., Korsgaard, N. J., Benn, D. I., Hewitt, I. J. & Fausto, R. S. A first constraint on basal melt-water production of the Greenland ice sheet. *Nature Communications* **12** (2021).

[37] Tsai, V. C. & Ruan, X. A simple physics-based improvement to the positive degree day model. *Journal of Glaciology* **64**, 661–668 (2018).

[38] Fausto, R., Mernild, S., Hasholt, B., Ahlstrøm, A. & Knudsen, N. Modeling suspended sediment concentration and transport, Mittivakkat glacier, southeast Greenland. *Arctic, Antarctic, and Alpine Research* **44**, 306–318 (2012).

[39] Cooper, M. G., Smith, L. C., Rennermalm, A. K., Miège, C., Pitcher, L. H., Ryan, J. C., Yang, K. & Cooley, S. W. Meltwater storage in low-density near-surface bare ice in the Greenland ice sheet ablation zone. *The Cryosphere* **12**, 955–970 (2018). URL https://tc.copernicus.org/articles/12/955/2018/.

[40] Schoof, C. Ice-sheet acceleration driven by melt supply variability. *Nature* **468**, 803–806 (2010).

[41] Flowers, G. E. Hydrology and the future of the Greenland Ice Sheet. *Nature Communications* **9** (2018).

[42] Meire, L., Mortensen, J., Rysgaard, S., Bendtsen, J., Boone, W., Meire, P. & Meysman, F. J. Spring bloom dynamics in a subarctic fjord influenced by tidewater outlet glaciers (Godthåbsfjord, SW Greenland). *Journal of Geophysical Research: Biogeosciences* **121**, 1581–1592 (2016).

[43] Carroll, D., Sutherland, D. A., Shroyer, E. L., Nash, J. D., Catania, G. A. & Stearns, L. A. Subglacial discharge-driven renewal of tidewater glacier fjords. *Journal of Geophysical Research: Oceans* **122**, 6611–6629 (2017).

[44] Moon, T., Sutherland, D. A., Carroll, D., Felikson, D., Kehrl, L. & Straneo, F. Subsurface iceberg melt key to Greenland fjord freshwater budget. *Nature Geoscience* **11** (2018).

[45] Cape, M. R., Straneo, F., Beaird, N., Bundy, R. M. & Charette, M. A. Nutrient release to oceans from buoyancy-driven upwelling at Greenland tidewater glaciers. *Nature Geoscience* **12** (2019).

[46] Torsvik, T., Albretsen, J., Sundfjord, A., Kohler, J., Sandvik, A. D., Skarðhamar, J., Lindbäck, K. & Everett, A. Impact of tidewater glacier retreat on the fjord system: Modeling present and future circulation in Kongsfjorden, Svalbard. *Estuarine, Coastal and Shelf Science* **220**, 152–165 (2019).

[47] Goelzer, H., Nowicki, S., Payne, A., Larour, E., Seroussi, H., Lipscomb, W. H., Gregory, J., Abe-Ouchi, A., Shepherd, A., Simon, E., Agosta, C., Alexander, P., Aschwanden, A., Barthel, A., Calov, R., Chambers, C., Choi, Y., Cuzzone, J., Dumas, C., Edwards, T., Felikson, D., Fettweis, X., Golledge, N. R., Greve, R., Humbert, A., Huybrechts, P., Clec'H, S. L., Lee, V.,

Leguy, G., Little, C., Lowry, D., Morlighem, M., Nias, I., Quiquet, A., Rückamp, M., Schlegel, N. J., Slater, D. A., Smith, R., Straneo, F., Tarasov, L., Wal, R. V. D. & Broeke, M. V. D. The future sea-level contribution of the Greenland ice sheet: A multi-model ensemble study of ISMIP6. *Cryosphere* **14**, 3071–3096 (2020).

[48] Fenty, I., Willis, J. K., Khazendar, A., Dinardo, S., Forsberg, R., Fukumori, I., Holland, D., Jakobsson, M., Moller, D., Morison, J. *et al.* Oceans Melting Greenland: Early results from NASA's ocean-ice mission in Greenland. *Oceanography* **29**, 72–83 (2016).

[49] Shreve, R. L. Movement of Water in Glaciers. *Journal of Glaciology* **11**, 205–214 (1972).

[50] How, P., Abermann, J., Ahlstrøm, A., A.P., S.B., B., J.E., Citterio, M., Colgan, W., Fausto, R., Karlsson, N., Jakobsen, J., Langley, K., Larsen, S., Lund, M., Mankoff, K., Pedersen, A., Rutishauser, A., Shields, C., Solgaard, A., van As, D., Vandecrux, B. & Wright, P. PROMICE and GC-Net automated weather station data in Greenland (2022).

[51] Lea, J. M. The Google Earth Engine Digitisation Tool (GEEDiT) and the Margin change Quantification Tool (MaQiT) – simple tools for the rapid mapping and quantification of changing Earth surface margins. *Earth Surface Dynamics* **6**, 551–561 (2018).